Design and development of an energy monitoring and SDCard–based data logging system for on-grid solar power plants

Alberta Bihaqil Hakiki[1], *Aldo* Febriyan[1], *Rizky* Aditya Fujiyanto[1], *As'ad* Shidqy Aziz[1*], *Aditya* Chandra Hermawan[1]

[1]Department of Electrical Engineering, Faculty of Vocational Studies, Universitas Negeri Surabaya, Surabaya, East Java, Indonesia

Abstract. This research aims to design and build a real-time energy monitoring and data logger tool using an ESP-32 microcontroller and displayed in home assistant software. Real-time monitoring of solar power plant performance is crucial for analyzing daily performance and making technical adjustments to optimize energy production, even under variable environmental condition. To overcome the problems in accuracy and real-time data recording, a system is needed that continuously monitors data based on a data logger. This system consists of several components including the PZEM-004T sensor, a real-time clock module, and an SD card module that are integrated into one system. Data retrieval in the system that has been created is done automatically in real-time and then saved in CSV format. Testing in this study has been successfully carried out with the lowest error value obtained in the R phase test of 0.13% and an accuracy value of 99.87%. While the lowest error value in the current test was obtained in the T phase test of 0.41% and an accuracy value of 99.59%. Meanwhile, the lowest error value in the power test was obtained in the T phase test of 0.10% and an accuracy value of 99.9%.

1 Introduction

The need for clean and renewable energy is growing alongside the expansion of industries and economic development. At the same time, global worries about environmental pollution, climate change, and the depletion of fossil fuels are on the rise[1–5]. Solar power provides a plentiful, dependable, eco-friendly, and widely available answer to the world's energy issues. As the main source of all renewable energy, the sun stands as the most powerful resource available to humanity[6–10]. Photovoltaic (PV) technology is essential for harnessing solar energy, presenting a sustainable answer to the growing global need for clean electricity[11,12]. PV systems convert sunlight directly into electrical power through semiconductor materials, delivering a dependable and environmentally friendly energy source without producing greenhouse gases or harmful pollutants[13–18].

Transitioning from fossil fuels to renewable energy systems (RES) poses a significant challenge for sectors like oil and natural gas extraction and processing. While green electricity has the potential to improve environmental sustainability, energy generation methods from existing renewable sources often require higher operating costs than conventional fossil-fuel-based systems. In addition, the power produced by solar panels is affected by such environmental factors as solar light intensity, the accumulation of dust, temperature, and fluctuating weather [19–28].

Real-time monitoring of solar power plant performance is crucial. Real-time data allows managers to analyze daily performance and make technical adjustments to maintain maximum energy production even under fluctuating environmental conditions [29–32]. Ideally, this data is transmitted instantly from the source to the destination platform without delay. Currently, monitoring methods are still performed manually, making them vulnerable to human error, equipment damage, and data inaccuracies[33,34]. To address these issues, an automated data logger-based monitoring system is needed to ensure the accuracy and continuity of data recording[35,36]

One technology widely used in monitoring systems is the data logger. A data logger is an electronic device capable of recording various environmental parameters such as temperature, wind speed, gas concentration, and electrical quantities (current and voltage) through electronic or electromechanical sensors, then storing them in memory. In its implementation, data loggers support various data storage and transmission methods, such as SD Cards, SMS Gateways, LAN (Local Area Network) systems, SCADA (Supervisory Control and Data Acquisition), and most recently using the Internet of Things[37–41].

The Internet of Things (IoT) is the idea that various physical devices (such as sensors, tools, machines, or everyday items) are connected to the internet and can communicate with each other and exchange data without direct human intervention[42,43]. IoT brings significant changes with benefits such as efficiency, automation, and ease of access. However, data security and device compatibility remain challenges that need to be addressed. As technology advances, IoT will increasingly strengthen its role in various sectors of life[44–48].One of the devices that can be used to

* Corresponding author: asadaziz@unesa.ac.id

© The Authors, published by EDP Sciences. This is an open access article distributed under the terms of the Creative Commons Attribution License 4.0 (https://creativecommons.org/licenses/by/4.0/).

implement the Internet of Things is the ESP 32. The ESP32 is a technological development that includes Wi-Fi and Bluetooth modules, so it has an excellent way of working with IoT systems. In the case of the ESP32, the Xtensa LX6 32-bit dual-core processor is a version that operates at MHz, with 520 KB of SRAM memory, and also a maximum of 16 MB of flash storage, so that it covers the time of supervision is a necessary task, such as real-time monitoring[49].

One of the studies discussing the application of data loggers using IoT. This paper introduces a novel open-source data logger system designed for real-time monitoring and fault detection during bench testing of combustion and electric engines. The system employs various sensors, including accelerometers, microphones, thermocouples, and gas sensors, to capture data on parameters like vibration, sound, temperature, and CO2 levels, crucial for identifying engine anomalies[50]. In the tests carried out, the researchers developed an Arduino Uno–based data logger system to monitor the performance of a Solar Power Plant with specific measurement parameters, while also evaluating the performance of the PZEM-004T sensor in recording data, which was then transmitted and visualized through the Thingspeak platform[51]. However, the study had some limitations, particularly regarding the use of a less flexible microcontroller. The Arduino Uno, which was used in the system, has limitations in terms of memory, processor speed, and connectivity capacity, restricting its ability to run parallel processes or handle complex data processing[52]. Additionally, the system lacked a data backup mechanism in the event of an internet connection failure, creating the risk of data loss when real-time transmission to the platform was disrupted.

This research contributes an automated, real-time energy monitoring and SDCard-based data logging system for on-grid solar power plants, addressing issues of data accuracy and continuity through an ESP-32 microcontroller, PZEM-004T sensor, and integration with Home Assistant. The study proposed the development of the monitoring Solar Power Plant system by adding backup data features through sd card. Adding a backup feature aims to create a data backup so that we can use the previous history along an open source platform, the home assistant. With this integration, systems are not only able to view energy data in real-time, and energy consumption within a given period.

2 Method

Based on Figure 1, the implementation method in this project begins with problem identification, namely the need for an efficient and integrated energy monitoring and location tracking system for On Grid Solar Power Plants. Next, a literature study was conducted to explore references and technical approaches from relevant previous research. After that, the main components were selected such as the ESP32 microcontroller, PZEM004T and ACS712 energy sensors, GPS modules, RTC, and SD Card. These components were then identified in detail to ensure their compatibility and functionality. The next stage is system design, including circuit design, data logger structure, and integration with the Home Assistant platform. Once the design has been finalized, the device is constructed in line with the design prepared. The next step in the project involves post instrumentation of the constructed system to establish its performance. Testing is then carried out to make sure the device works as expected in real condition.

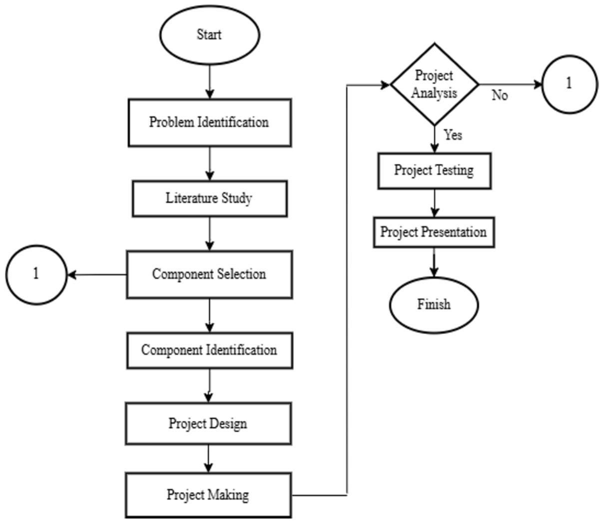

Fig. 1. Project creation method.

The data was collected through quantitative data collection methods. The data is numerical and directly measured from sensors recording of voltage, current, power, energy, and frequency which are automated and monitored at intervals. This data is automatically and continuously recorded by a data logger system and then stored in CSV format for further analysis. This approach allows for objective, consistent, and accurate monitoring of the performance of the developed IoT-based energy monitoring system.

2.1 Testing procedure

The results of the prototype design can be seen in Figure 3. The testing stage aims to test the performance of the designed system to see whether it is in accordance with what has been planned. The main stages in this test are integrating the PZEM 004T sensor and data logger, testing data collection, and storing data in a MicroSD card every 10 minute. Next, the integration between the MQTT broker and the home assistant software was tested to ensure data from the PZEM 004T sensor can be sent and displayed accurately. Finally, the data results obtained from storage on the SDCARD, including voltage current and power, will be compared with the measurement results using a Clamp meter to calculate the accuracy of the monitoring data results obtained.

2.2 Electrical energy parameter

Calculation the PZEM-004T sensor was tested to ensure its ability to accurately read electrical parameters such as voltage (volts), current (amperes), active power (watts), frequency (Hz), and energy (kWh) on each phase in a 3-phase electrical system. This project used three PZEM-004T sensors, connected to the R, S, and T phases, respectively. The test used an Clamp Meter as a comparator to calculate the error difference and accuracy. To calculate error and accuracy respectively can be seen in equation 1 and equation 2.

$$Error\% = \left(\frac{PZEM\ Value - Reference\ Value}{Reference\ Value}\right) \times 100\% \quad (1)$$

$$Accuracy = 100\% - Error\% \quad (2)$$

3 System design

The Fig. 2 shows the wiring arrangement of the three-phase electrical energy monitoring and data recording system based on ESP32. The system consists of three PZEM-004T v3.0 energy sensors, each of which is used to measure electrical parameters (voltage, current, power, frequency, and energy) in the R, S, and T phases. For time recording, the DS3231 RTC module is used which is connected via the I2C line (SDA and SCL) to synchronize the data recording time in real-time. As for data storage, the system uses a microSD card module connected through the SPI interface, which functions to store the measurement data into a CSV file that is differentiated at each time (every 10 minutes). The ESP32 is also connected to a WiFi network and functions to periodically send data to the Home Assistant server via the MQTT protocol, as well as running a simple web server feature to make it easier for users to access and download data directly without having to unplug the SD Card from the device. This wiring array supports a real-time three-phase energy monitoring system, automatic data recording, and easy access and processing of data for analysis and reporting purposes.

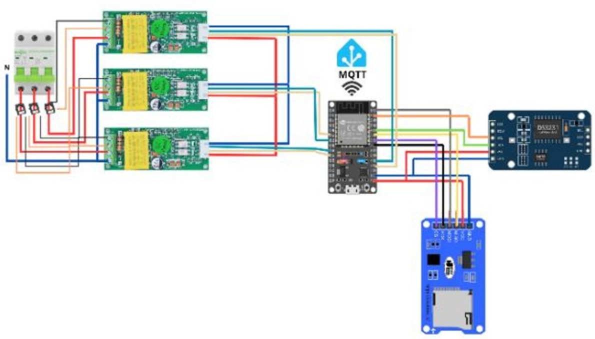

Fig. 2. Project design.

4 Result and discussion

4.1 Prototipe design

After the design and assembly process is completed, the hardware system for energy monitoring, and the data logger for the solar system are successfully built. The system consists of several main components assembled in an integrated manner, namely the ESP32 microcontroller, three PZEM-004T sensors, the ACS712 current sensor, the DC voltage sensor, RTC, micro SD, and the 20x4 I2C LCD display. In addition, there are additional materials such as breadboard and jumper cables. The system also comes with a WiFi connection that allows integration into the Home Assistant platform for real-time remote monitoring. The image below shows that the hardware was successfully assembled and tested functionally. The ESP32 is capable of reading all sensors simultaneously and automatically setting the display of information on the LCD. This series shows that all components have worked according to their respective functions. The testing process is also carried out to ensure that there are no connection errors or data readings. The results of the prototype assembly can be seen in Fig 3.

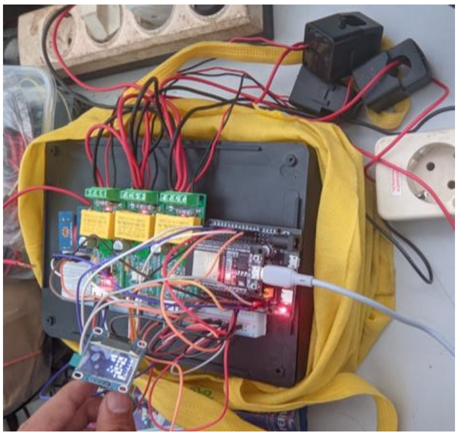

Fig. 3. Energy monitoring prototype.

4.2 Monitoring results on home assistant

The integration of the solar power plant monitoring system into Home Assistant is carried out using the MQTT communication protocol, where the ESP32 acts as a data sender from the PZEM-004T, ACS712, and DC voltage sensors. Before Home Assistant receives data, a YAML configuration is first performed so that it can be used as an entity to display the data. The obtained data is packaged in JSON format and sent to the MQTT broker (Mosquitto) that has been configured in Home Assistant. This configuration allows Home Assistant to automatically receive and display data on the dashboard in the form of numbers through setting certain topics. With this visual display, users can monitor electrical parameters such as voltage, current, power, and energy in real-time and remotely through various devices such as smartphones or computers. Fig 4 shows the Home Assistant reading results.

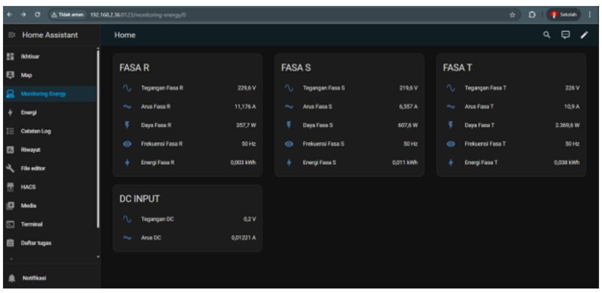

Fig. 4. Home assistant reading results.

4.3 Voltage data testing on the RST phase

This test is conducted by comparing the results obtained by the sensor PZEM-004T stored on an SD card with direct measurements using a clamp meter. This test aims to determine the accuracy of the energy monitoring data read by the PZEM-004T sensor and stored on the SD card. The data to be measured for accuracy voltage of RST Phase. The results of comparing the data obtained on the SD CARD with measurements using a clamp meter on the R Phase, S Phase and T Phase respectively can be seen in Fig 5, Fig 6 and Fig 7.

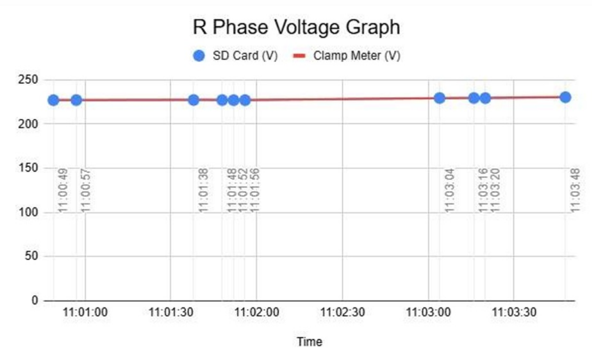

Fig. 5. R phase voltage graph.

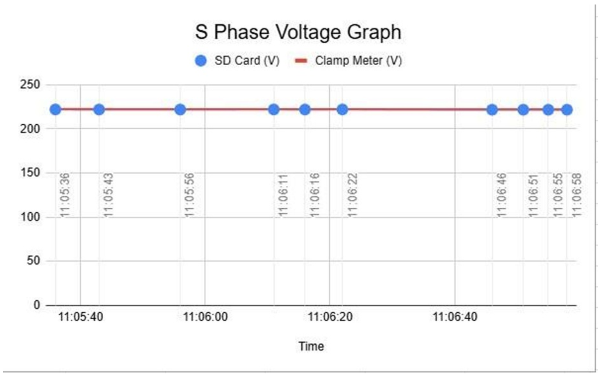

Fig. 6. S phase voltage graph.

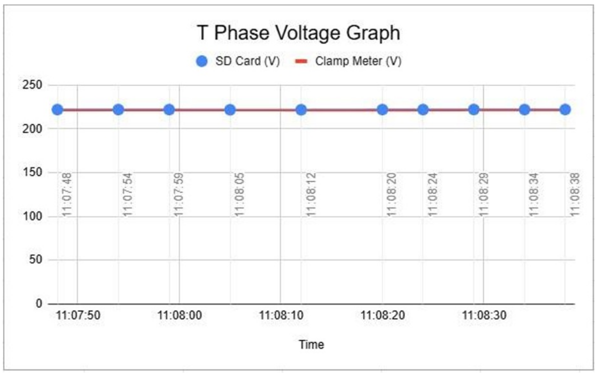

Fig. 7. T phase voltage graph.

The data results from the three phase RST voltages that can be found show that the PZEM-004T sensor readings are accurate when compared to measurements using an ampere clamp. This can be seen in table 1 with an average error value of the R phase voltage of 0.13%, the S phase voltage of 0.24%, and the T phase voltage of 0.28% from sampling of 10 data on each phase. Meanwhile, the tolerance value of the PZEM-004T sensor is 0.5%.

4.4 Current data testing on the RST phase

This test was conducted by comparing the current measurement results on the RST phase obtained from the PZEM-004T sensor stored on an SD card with the results of direct measurements using a clamp meter. This test aims to determine the accuracy of the current monitoring data read by the PZEM-004T sensor and stored on the SD card.

The results of the comparison of data obtained on the SD card with the results of measurements using a clamp meter on the R Phase, S Phase, and T Phase respectively can be seen in Fig 8, Fig 9 and Fig 10.

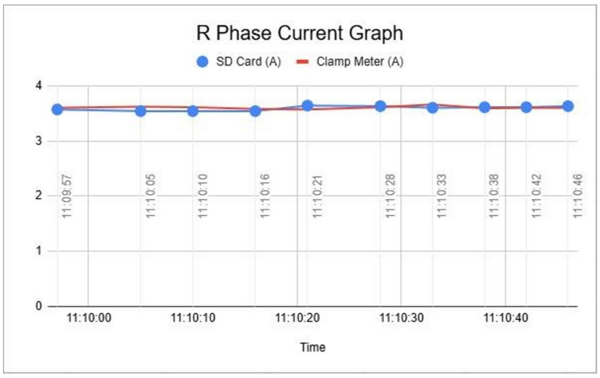

Fig. 8. R phase current graph.

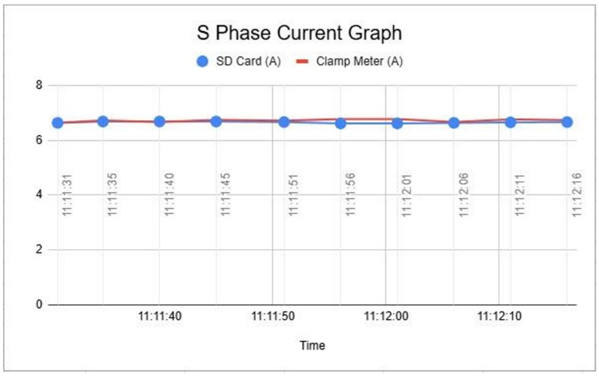

Fig. 9. S phase current graph.

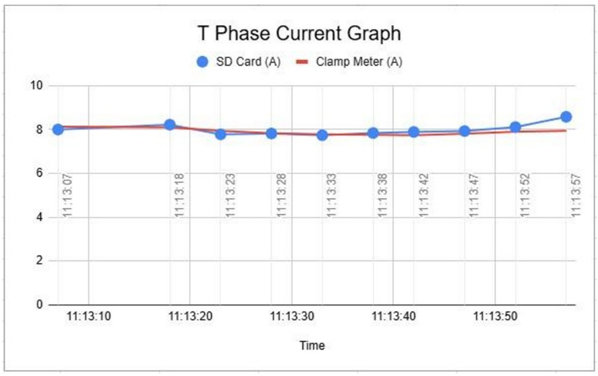

Fig. 10. T phase current graph.

The data obtained from the three currents in the RST phase produced shows that the PZEM-004T sensor readings are accurate when compared to measurements using a Clamp meter. However, there are several sensors with high error values, which exceed the PZEM-004T sensor tolerance limit of 0.5%. This can be seen from the table and graph above, the average error value of the R current is 0.69%, the S current is 0.67%, and the T current is 0.41%.

4.5 Power data testing on the RST phase

This test is conducted by comparing the power measurement results on the RST phase obtained from the PZEM-004T sensor stored on the SD card with the theoretical calculation results. The theoretical calculation for electrical power can be seen in equation 3.

$$P = V \times I \times cos\vartheta \qquad (3)$$

This test aims to determine the accuracy of the power monitoring data read by the PZEM-004T sensor and stored on the SD card. The results of the comparison of the data obtained on the SD card with the results of measurements using a clamp meter on the R Phase, S Phase, and T Phase, respectively, can be seen in Fig 11, Fig 12, and Fig 13.

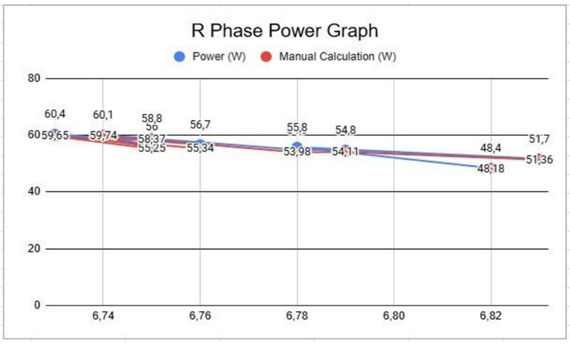

Fig. 11. R phase power graph.

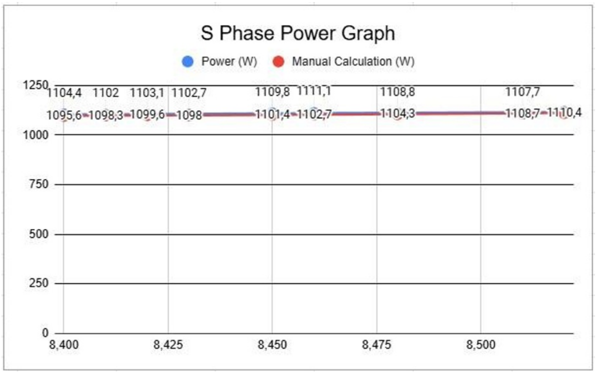

Fig. 12. S phase power graph.

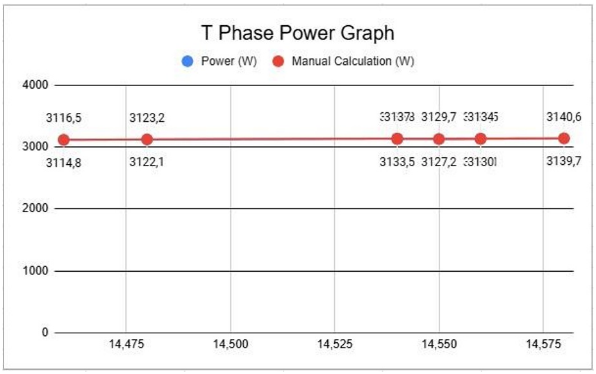

Fig. 13 T phase power graph.

Based on the graphs in Fig 11, Fig 12, and Fig 13, the power readings obtained from the RST phase show that the PZEM-004T sensor is accurate when compared with theoretical calculations using Equation 3. With an average error value of R power of 1.09%, S power of 0.83%, and T power of 0.10%. Details of the comparison data for the power stored on the SD card with theoretical calculations can be seen in Table 3.

Table 1. RST phase voltage.

No	R Phase				S Phase				T Phase			
	Time	SD Card V	Clamp Meter V	Error	Time	SD Card V	Clamp Meter V	Error	Time	SD Card V	Clamp Meter V	Error
1	11:00:49	227	227,2	0,088	11:05:36	222	222,4	0,179	11:07:48	222	221,2	0,362
2	11:00:57	227,1	227,2	0,044	11:05:43	221,9	222,4	0,224	11:07:54	222	221,2	0,362
3	11:01:38	227,2	227,5	0,131	11:05:56	221,9	222,3	0,179	11:07:59	222	221,2	0,362
4	11:01:48	227,1	227,5	0,175	11:06:11	222	222,3	0,134	11:08:05	221,8	221,2	0,271
5	11:01:52	227	227,6	0,263	11:06:16	221,9	222,4	0,224	11:08:12	221,8	221,1	0,317
6	11:01:56	227	227,3	0,131	11:06:22	222	222,3	0,134	11:08:20	222	221,1	0,407
7	11:03:04	229,4	229,1	0,130	11:06:46	221,7	222,1	0,180	11:08:24	222	221,1	0,407
8	11:03:16	229,4	229,6	0,087	11:06:51	221,7	222,1	0,180	11:08:29	222,1	221,3	0,362
9	11:03:20	229,3	229,7	0,174	11:06:55	221,7	222,1	0,180	11:08:34	222	221,3	0,316
10	11:03:48	230,3	230,6	0,130	11:06:58	221,7	222	0,135	11:08:38	222,1	221,3	0,362

Table 2. RST phase current.

No	R Phase				S Phase				T Phase			
	Time	SD Card A	Clamp Meter A	Error	Time	SD Card A	Clamp Meter A	Error	Time	SD Card A	Clamp Meter A	Error
1	11:09:57	3,57	3,6	0,833	11:11:31	6,63	6,63	0	11:13:07	8	8,13	1,599
2	11:10:05	3,54	3,62	2,210	11:11:35	6,68	6,72	0,595	11:13:18	8,22	8,10	1,481
3	11:10:10	3,54	3,61	1,939	11:11:40	6,68	6,66	0,300	11:13:23	7,78	7,94	2,015
4	11:10:16	3,54	3,58	1,117	11:11:45	6,68	6,74	0,890	11:13:28	7,82	7,83	0,127
5	11:10:21	3,64	3,57	1,960	11:11:51	6,66	6,71	0,745	11:13:33	7,74	7,78	0,514
6	11:10:28	3,63	3,61	0,554	11:11:56	6,61	6,77	2,363	11:13:38	7,84	7,76	1,030
7	11:10:33	3,6	3,66	1,639	11:12:01	6,61	6,77	2,363	11:13:42	7,89	7,74	1,937
8	11:10:38	3,61	3,59	0,557	11:12:06	6,63	6,66	0,450	11:13:47	7,93	7,81	1,536
9	11:10:42	3,61	3,6	0,278	11:12:11	6,65	6,76	1,627	11:13:52	8,11	7,90	2,658
10	11:10:46	3,63	3,6	0,833	11:12:16	6,66	6,73	1,040	11:13:57	8,58	7,94	8,060

Table 3. RST phase power.

No	R Phase				S Phase				T Phase			
	Power (W)	Theoretical (W)	Error (%)	Accuracy (%)	Power (W)	Theoretical (W)	Error (%)	Accuracy (%)	Power (W)	Theoretical (W)	Error (%)	Accuracy (%)
1	56,7	55,34	2,46%	99,54%	1109	1108,7	0,14%	99,86%	3136,5	3132,1	0,14%	99,86%
2	60,4	59,65	1,26%	98,74%	1107,7	1108,7	0,14%	99,86%	3140,6	3139,7	0,03%	99,97%
3	56	55,25	1,36%	98,64%	1108,8	1104,3	0,64%	99,36%	3134,2	3128,6	0,18%	99,82%
4	60,1	59,74	0,60%	99,40%	1102,7	1098	0,68%	99,32%	3134	3130,0	0,13%	99,87%
5	58,8	58,37	0,74%	99,26%	1111,1	1102,7	2,46%	97,54%	3129,7	3127,2	0,08%	99,92%
6	54,9	53,98	1,70%	98,30%	1116,7	1110,4	0,84%	99,16%	3133,4	3127,2	0,20%	99,80%
7	54,8	54,11	1,28%	98,72%	1109,8	1101,4	1,00%	99,00%	3116,5	3114,8	0,05%	99,95%
8	51,7	51,36	0,66%	99,34%	1104,4	1095,6	1,02%	98,98%	3123,2	3122,1	0,04%	99,96%
9	55,8	55.6	0,36%	99,64%	1102	1098,3	0,635	99,37%	3135,8	3134,1	0,05%	99,95%
10	48,4	48,18	0,46%	99,54%	1103,1	1099,6	0,71%	99,29%	3137	3133,5	0,11%	99,89%
	Average		1,09%	98,91%	Average		0,83%	99,17%	Average		0,10%	99,90%

5 Conclusion

In the assembly and testing stage of the project, it has been possible to make an energy monitoring system, and data logger on solar PV, in the manufacture it has been successful and functions well. From the test results, it is quite good even though there is still a difference above the tolerance limit. Data can also be backed up to micro SD in the form of a CSV file. In addition, it can also be integrated into the Home Assistant through the MQTT protocol to display data on the dashboard in real time. Although the system shows good performance, further research can be focused on improving sensor calibration or data processing algorithms to achieve higher precision.

References

1. Omri A, Jabeur S Ben, Climate policies and legislation for renewable energy transition: the roles of financial sector and political institutions. Technol Forecast Soc Change, **203**, 123347 (2024). https://doi.org/10.1016/j.techfore.2024.123347
2. Sofian ADABA, Lim HR, Munawaroh HSH, Ma Z, Chew KW, Show PL, Machine learning and the renewable energy revolution: exploring solar and wind energy solutions for a sustainable future including innovations in energy storage. Sustainable Development, **32**, 3953–78 (2024). https://doi.org/10.1002/sd.2885
3. Arief R, Maulana MIF, Current and voltage monitoring in wind power plants using ESP8266 and Node-Red. Vokasi Unesa Bulletin of

Engineering, Technology and Applied Science, **1**, 72–80 (2024). https://doi.org/10.26740/vubeta.v1i2.35429

4. Ukoba K, Olatunji KO, Adeoye E, Jen T, Madyira DM, Optimizing renewable energy systems through artificial intelligence: review and future prospects. Energy & Environment, **35**, 3833–79 (2024). https://doi.org/10.1177/0958305x241256293
5. Omri A, Jabeur S Ben, Climate policies and legislation for renewable energy transition: the roles of financial sector and political institutions. Technol Forecast Soc Change, **203**, 123347 (2024). https://doi.org/10.1016/j.techfore.2024.123347
6. He X, Khan S, Öztürk İ, Murshed M, The role of renewable energy investment in tackling climate change concerns: environmental policies for achieving SDG-13. Sustainable Development, **31**, 1888–901 (2023). https://doi.org/10.1002/sd.2491
7. Wei S, Jiandong W, Saleem H, The impact of renewable energy transition, green growth, green trade and green innovation on environmental quality: evidence from top 10 green future countries. Front Environ Sci, **10**, (2023). https://doi.org/10.3389/fenvs.2022.1076859
8. Yu J, Tang YM, Chau KY, Nazar R, Ali S, Iqbal N, Role of solar-based renewable energy in mitigating CO2 emissions: evidence from quantile-on-quantile estimation. Renew Energy, **182**, 216–26 (2022). https://doi.org/10.1016/j.renene.2021.10.002
9. Chen L, Hu Y, Wang R, Li X, Chen Z, Hua J, et al, Green building practices to integrate renewable energy in the construction sector: a review. Environ Chem Lett, **22**, 751–84 (2023). https://doi.org/10.1007/s10311-023-01675-2
10. Wei P, Abid M, Adun H, Awoh DK, Cai D, Zaini J, et al, Progress in energy storage technologies and methods for renewable energy systems application. Applied Sciences, **13**, 5626 (2023). https://doi.org/10.3390/app13095626
11. Worku AK, Ayele DW, Deepak DB, Gebreyohannes AY, Agegnehu SD, Kolhe ML, Recent advances and challenges of hydrogen production technologies via renewable energy sources. Advanced Energy and Sustainability Research, **5**, (2024). https://doi.org/10.1002/aesr.202300273
12. Adebayo TS, Ullah S, Towards a sustainable future: the role of energy efficiency, renewable energy, and urbanization in limiting CO2 emissions in Sweden. Sustainable Development, **32**, 244–59 (2023). https://doi.org/10.1002/sd.2658
13. Murtaza H, Ain Q, Munir J, Ghaithan HM, Ahmed AAA, Aldwayyan AS, et al, A DFT approach to explore the structural, optoelectronic, mechanical, and thermoelectric attributes of lead-free RbInX3 (X = I, Br, Cl) halide perovskites for renewable energy applications. Phys Scr, **99**, 055947 (2024). https://doi.org/10.1088/1402-4896/ad35ee
14. Nazir A, Dixit A, Khera EA, Manzoor M, Sharma R, Moayad AJA, A DFT exploration of the optoelectronic and thermoelectric features of a novel halide double perovskite A2YAuI6 (A = Rb, Cs) for solar cell and renewable energy applications. Mater Adv, **5**, 4262–75 (2024). https://doi.org/10.1039/d4ma00090k
15. Moshwan R, Shi X, Zhang M, Yue Y, Liu W, Li M, et al, Advances and challenges in hybrid photovoltaic-thermoelectric systems for renewable energy. Appl Energy, **380**, 125032 (2025). https://doi.org/10.1016/j.apenergy.2024.125032
16. Wang Y, Wang R, Tanaka K, Ciais P, Peñuelas J, Balkanski Y, et al, Accelerating the energy transition towards photovoltaic and wind in China. Nature, **619**, 761–7 (2023). https://doi.org/10.1038/s41586-023-06180-8
17. Green MA, Dunlop ED, Yoshita M, Kopidakis N, Bothe K, Siefer G, et al, Solar cell efficiency tables (version 62). Progress in Photovoltaics Research and Applications, **31**, 651–63 (2023). https://doi.org/10.1002/pip.3726
18. Wei S, Jiandong W, Saleem H, The impact of renewable energy transition, green growth, green trade and green innovation on environmental quality: evidence from top 10 green future countries. Front Environ Sci, **10**, (2023). https://doi.org/10.3389/fenvs.2022.1076859
19. Kabeyi MJB, Olanrewaju OA, Sustainable energy transition for renewable and low carbon grid electricity generation and supply. Front Energy Res, **9**, (2022). https://doi.org/10.3389/fenrg.2021.743114
20. Messini EMB, Bourek Y, Ammari C, Zouaghi A, Pace L, Optimization and decision-making approach for energy storage strategies in a natural gas processing facility with photovoltaic renewable energy supply. J Energy Storage, **112**, 115431 (2025). https://doi.org/10.1016/j.est.2025.115431
21. Liu J, Hu H, Yu SS, Trinh H, Virtual power plant with renewable energy sources and energy storage systems for sustainable power grid-formation, control techniques and demand response. Energies (Basel), **16**, 3705 (2023). https://doi.org/10.3390/en16093705
22. Blaabjerg F, Yang Y, Kim KA, Rodríguez J, Power electronics technology for large-scale renewable energy generation. Proceedings of the IEEE, **111**, 335–55 (2023). https://doi.org/10.1109/jproc.2023.3253165
23. Hossain MK, Samajdar DP, Das RC, Arnab AA, Rahman MdF, Rubel MHK, et al, Design and simulation of Cs2BiAgI6 double perovskite solar cells with different electron transport layers for efficiency enhancement. Energy & Fuels, **37**, 3957–79 (2023). https://doi.org/10.1021/acs.energyfuels.3c00181
24. Yang L, Zhou H, Duan Y, Wu M, He K, Li Y, et al, 25.24%-efficiency FACsPbI3 perovskite solar cells enabled by intermolecular esterification reaction of DL-carnitine hydrochloride. Advanced Materials,

35, (2023). https://doi.org/10.1002/adma.202211545
25. Sofian ADABA, Lim HR, Munawaroh HSH, Ma Z, Chew KW, Show PL, Machine learning and the renewable energy revolution: exploring solar and wind energy solutions for a sustainable future including innovations in energy storage. Sustainable Development, **32**, 3953–78 (2024). https://doi.org/10.1002/sd.2885
26. Devlin A, Kossen J, Goldie-Jones H, Yang A, Global green hydrogen-based steel opportunities surrounding high quality renewable energy and iron ore deposits. Nat Commun, **14**, (2023). https://doi.org/10.1038/s41467-023-38123-2
27. Mahmood Y, Afrin T, Huang Y, Yodo N, Sustainable development for oil and gas infrastructure from risk, reliability, and resilience perspectives. Sustainability, **15**, 4953 (2023). https://doi.org/10.3390/su15064953
28. Delfianti R, Tazayul VA, Mustaqim B, Nusyura F, Harsito C, Internet of Things (IoT) based electrical power monitoring system for solar power plants using Telegram application. Vokasi Unesa Bulletin of Engineering, Technology and Applied Science, **2**, 428–43 (2025). https://doi.org/10.26740/vubeta.v2i3.39405
29. Rekeraho A, Cotfas DT, Cotfas PA, Tuyishime E, Bălan T, Acheampong R, Enhancing security for IoT-based smart renewable energy remote monitoring systems. Electronics (Basel), **13**, 756 (2024). https://doi.org/10.3390/electronics13040756
30. P. Sun, G. Kour, S. C. Lee, A. Lim, J. Park, and Y. Park, 25.58% efficiency of perovskite solar cells by interface engineering of thermally evaporated CsF in the SnO_2/perovskite layer. Appl Surf Sci. **668**, 162964 (2024). https://doi.org/10.1016/j.apsusc.2024.162964
31. Z. Liu, X. Deng, H. Peng, W. Lu, S. Li, J. Zhang, et al. Thermodynamic, spectroscopic and optoelectronic investigations of methylammonium and formamidinium-based perovskites for solar cells: a DFT study. Phys Chem Chem Phys. **26**, 1397–1408 (2024). https://doi.org/10.1039/d3cp04889c
32. R. Chauhan, R. Kumar, and N. Jena, Comparative investigation of hybrid organic–inorganic lead-free perovskites for optoelectronic applications: insights from DFT calculations. Comput Mater Sci. **236**, 112877 (2024). https://doi.org/10.1016/j.commatsci.2024.112877
33. P. Pooja, A. Kaur, P. Kumar, and K. Singh, Exploring structural, mechanical, optoelectronic and photovoltaic properties of inorganic perovskite-like A_2PdBr_6 (A = Cs, Rb, K). J Mater Sci Mater Electron. **35**, 5678–5692 (2024). https://doi.org/10.1007/s10854-024-13562-3
34. M. H. Rahman, S. K. Saha, and N. Amin, A comprehensive review of recent developments in tin halide perovskite solar cells: stability challenges and future perspectives. Sol Energy Mater Sol Cells. **259**, 112345 (2024). https://doi.org/10.1016/j.solmat.2024.112345
35. L. Zhao, X. Li, W. Yu, and J. Chen, Effect of compositional engineering on the stability of mixed halide perovskites. Mater Today Chem. **33**, 101857 (2024). https://doi.org/10.1016/j.mtchem.2024.101857
36. T. Nguyen, H. Tran, and D. Pham, Machine learning-guided discovery of lead-free perovskites for photovoltaic applications. npj Comput Mater. **10**, 135 (2024). https://doi.org/10.1038/s41524-024-01283-6
37. A. Banerjee, S. Das, and M. Roy, Influence of humidity on structural and electronic properties of hybrid perovskite $MAPbI_3$: a first-principles study. J Phys Chem C. **128**, 15423–15433 (2024). https://doi.org/10.1021/acs.jpcc.4c04321
38. R. M. Torres, F. J. Morales, and C. H. Vega, Defect passivation in perovskite solar cells via organic–inorganic interface modifiers. Chem Eng J. **495**, 155046 (2024). https://doi.org/10.1016/j.cej.2024.155046
39. D. Chandra, S. Yadav, and P. Singh, Halide mixing strategies for enhanced stability and bandgap tunability in lead halide perovskites. Mater Chem Front. **8**, 2204–2215 (2024). https://doi.org/10.1039/d4qm00097f
40. K. Yamashita, N. Ogawa, and T. Suzuki, Enhanced carrier mobility in 2D perovskite heterostructures with interlayer organic cations. ACS Appl Mater Interfaces. **16**, 25012–25020 (2024). https://doi.org/10.1021/acsami.4c03210
41. J. Park, S. H. Kim, and Y. H. Lee, Computational insights into the defect tolerance of formamidinium-based perovskites. J Phys Chem Lett. **15**, 4071–4078 (2024). https://doi.org/10.1021/acs.jpclett.4c00873
42. C. Gao, Z. Xu, and Q. Li, Band alignment and defect formation in Sn-based halide perovskites for lead-free solar cells. Phys Rev Mater. **8**, 045402 (2024). https://doi.org/10.1103/PhysRevMaterials.8.045402
43. L. Hu, X. Wang, and M. Zhao, Role of organic cations in the stability of hybrid perovskites under illumination. Adv Funct Mater. **34**, 2402863 (2024). https://doi.org/10.1002/adfm.202402863
44. Y. Zhang, J. Chen, and F. Liu, Defect chemistry and ionic migration in all-inorganic $CsPbBr_3$ perovskites. J Mater Chem A. **12**, 17124–17134 (2024). https://doi.org/10.1039/d4ta02219a
45. S. L. Nguyen, M. H. Pham, and T. Q. Tran, Electronic structure tuning of halide perovskites by B-site cation substitution: a first-principles study. J Alloys Compd. **975**, 173421 (2024). https://doi.org/10.1016/j.jallcom.2024.173421
46. H. S. Kim, Y. M. Kim, and J. H. Noh, Recent advances in defect passivation strategies for perovskite solar cells. Nano Energy. **117**, 109998

(2024). https://doi.org/10.1016/j.nanoen.2024.109998

47. F. Ahmed, M. Khan, and N. Islam, Charge carrier dynamics in doped perovskite films: insights from transient spectroscopy. Sol RRL. **8**, 2400389 (2024). https://doi.org/10.1002/solr.202400389
48. T. Ito, M. Kobayashi, and Y. Kawai, Photostability enhancement of perovskite thin films using passivating polymer coatings. ACS Appl Energy Mater. **7**, 11123–11131 (2024). https://doi.org/10.1021/acsaem.4c01512
49. R. Pandey, N. Gupta, and A. Sharma, Thermodynamic stability and defect energetics of halide perovskites under light soaking. Mater Today Phys. **40**, 101745 (2024). https://doi.org/10.1016/j.mtphys.2024.101745
50. W. Zhao, S. Chen, and X. Ren, Investigation of mixed halide perovskites: phase segregation and ion migration mechanisms. J Energy Chem. **97**, 302–312 (2024). https://doi.org/10.1016/j.jechem.2024.06.012
51. M. Das, T. Chakraborty, and R. Bose, Insights into moisture-induced degradation pathways of hybrid halide perovskites. Chem Mater. **36**, 8211–8222 (2024). https://doi.org/10.1021/acs.chemmater.4c02345
52. G. Liang, P. Zhou, and J. Wang, Role of interfacial dipoles in charge transport at the perovskite/electron transport layer interface. Small. **20**, 2401125 (2024). https://doi.org/10.1002/smll.202401125